Diagnosis of Lung Nodule Using Reinforcement Learning and Geometric Measures

Aristófanes Correâ Silva[1], Valdeci Ribeiro da Silva Junior[2], Areolino de Almeida Neto[1], and Anselmo Cardoso de Paiva[2]

[1] Federal University of Maranhão - UFMA, Department of Electrical Engineering
Av. dos Portugueses, SN, Campus do Bacanga, Bacanga
65085-580, São Luís, MA, Brazil
ari@dee.ufma.br, areolino@gmx.net

[2] Federal University of Maranhão - UFMA, Department of Computer Science
Av. dos Portugueses, SN, Campus do Bacanga, Bacanga
65085-580, São Luís, MA, Brazil
paiva@deinf.ufma.br, valdeci_jr@hotmail.com

Abstract. This paper uses a set of 3D geometric measures with the purpose of characterizing lung nodules as malignant or benign. Based on a sample of 36 nodules, 29 benign and 7 malignant, these measures are analyzed with a technique for classification and analysis called reforcement learning. We have concluded that this techinique allows good discrimination from benign to malignant nodules.

1 Introduction

Lung cancer is known as one of the cancers with shortest survival after diagnosis [1]. Therefore, the sooner it is detected the larger the patient's chance of cure. On the other hand, the more information physicians have available, the more precise the diagnosis will be.

In many cases, it is possible to characterize a nodule as malignant or benign by analyzing its shape. If the nodule is rounded or has a well defined shape, it is probably benign; if it is spiculated or has an irregular shape, it is probably malignant. Figure 1 exemplifies such characteristics. However, in some cases it is hard to distinguish malignant nodules from benign ones [2], [3].

To solve the nodule diagnosis problem we have in general a two phase approach. In the first phase we must extract nodules characteristics that must help us to differentiate the benign from malignant ones. Next phase is devoted to classify based on the extracted characteristics the nodules.

A common approach for the first phase are the model based techniques, that use mathematical to describe the characteristics of lung nodule and thefore how to find them is a set of images.

Statistical and learning based methods are commmonly applied to the second phase, such as discriminant analysis, neural network and reinforcement learning [4], [5], [6]. Learning-based methods are a promissing techniques, they

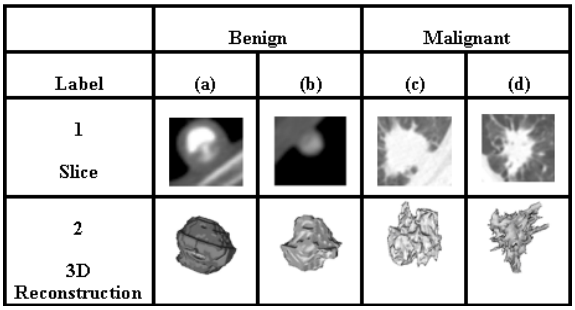

Fig. 1. Examples of benign lung nodules (a and b) and malignant lung nodules (c and d).

find out the characteristics from real images already classified as malignant ou benign and "learn" what can define a particular type of nodule.

The purpose of the present work is to investigate the adequacy of the reinforcement learning technique to classify lung nodules based on a set of 3D geometric measures extracted from the lung lesions Computerized Tomography (CT) images.

This paper is organized as follows. Section 2 describes the image database used in the paper, and discusses in detail the geometric measures used to discriminate lung nodules. Tests, discussion and analysis of the application of reinforcement learning to the nodules classification are treated in Section 4. Finally, Section 5 presents some concluding remarks.

2 Material and Methods

2.1 Image Acquisition

The images were acquired with a Helical GE Pro Speed tomography under the following conditions: tube voltage 120 kVp, tube current 100 mA, image size 512×512 pixels, voxel size $0.67 \times 0.67 \times 1.0$ mm. The images were quantized in 12 bits and stored in the DICOM format [7].

2.2 3D Extraction and Reconstruction of Lung Nodule

In most cases, lung nodules are easy to be visually detected by physicians, since their shape and location are different from other lung structures. However, the nodule voxel density is similar to that of other structures, such as blood vessels, which makes automatic computer detection difficult. This happens especially when a nodule is adjacent to the pleura. For these reasons, we have used the 3D region growing algorithm with voxel aggregation [8], which provides physicians greater interactivity and control over the segmentation and determination of required parameters (thresholds, initial slice and seed).

The Marching Cubes algorithm [9] is used to build an explicit representation of volume data. The measures described along the present paper will use this representation. In order to remove irregularities of the reconstructed surface, the Laplacian smoothing technique [10] is used. Figures 2 (a) and (b) show the result of applying the Marching Cubes algorithm and the Laplacian technique, respectively.

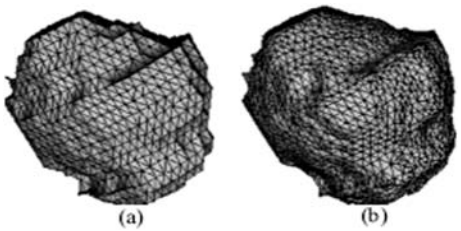

Fig. 2. (a)Application of Marching Cubes. (b) Application of Laplacian technique.

2.3 3D Geometric Measures

The measures to be presented in this section seek to capture information on the nodule's 3D geometry from the CT. The measures should ideally be invariant to changes in the image's parameters, such as voxel size, orientation, and slice thickness.

Sphericity Index: The Sphericity Index (SI) measures the nodule's behavior in relation to a spherical object. It is defined as

$$SI = \frac{6\sqrt{\pi}V}{A^{\frac{3}{2}}} \tag{1}$$

where V is the surface volume and A corresponds to the surface area. Thus, if the nodule's shape is similar to a sphere, the value will be close to 1. In all cases, $SI \leq 1$.

Convexity Index: The Convexity Index (CI) [11] measures the degree of convexity, defined as the area of the surface of object B $(A(B))$ divided by the area of the surface of its convex hull ($A(H_B)$). That is,

$$CI = \frac{A(B)}{A(H_B)} \tag{2}$$

The more convex the object is, the closer the value of CI will be to 1. For all objects, $CI \geq 1$.

Curvature Index: The two measures presented below are based on the main curvatures k_{min} and k_{max}, defined by

$$k_{\min,\max} = H \mp \sqrt{H^2 - K} \tag{3}$$

where K and H are the Gaussian and mean curvatures, respectively. The values of H and K are estimated using the methods described in [12].

a) Intrinsic curvature: The Intrinsic Curvature Index (ICI) [11], [12] captures information on the properties of the surface's intrinsic curvatures, and is defined as

$$ICI = \frac{1}{4\pi} \int\int |k_{\min} k_{\max}| dA \tag{4}$$

Any undulation or salience on the surface with the shape of half a sphere increments the Intrinsic Curvature Index by 0.5, regardless of its size - that is, the ICI counts the number of regions with undulations or saliences on the surface being analyzed.

b) Extrinsic curvature: The Extrinsic Curvature Index (ECI) [11], [12] captures information on the properties of the surface's extrinsic curvatures, and is defined as

$$ECI = \frac{1}{4\pi} \int\int |k_{\max}| \left(|k_{\max}| - |k_{\min}|\right) dA \tag{5}$$

Any crack or gap with the shape of half a cylinder increments the ECI in proportion to its length, starting at 0.5 if its length is equal to its diameter - that is, the ECI counts the number and length (in relation to the diameter) of semicylindrical cracks or gaps on the surface.

Types of Surfaces: With the values of extrinsic (H) and intrinsic (K) curvatures, it is possible to specify eight basic types of surfaces [13], [14]: *peak* ($K > 0$ and $H < 0$), *pit* ($K > 0$ and $H > 0$), *ridge* ($K = 0$ and $H < 0$), *flat* ($K = 0$ and $H = 0$), *valley* ($K = 0$ and $H > 0$), *saddle valley* ($K < 0$ and $H > 0$), *minimal* ($K < 0$ and $H = 0$), *saddle ridge* ($K < 0$ and $H < 0$).

The measures described below were presented in [15] for the classification of lung nodules and the results were promising. However, they have computed curvatures H and K directly from the voxel intensity values, while here we compute them in relation to the extracted surface, which is composed by triangles.

In practice, it is difficult to determine values that are exactly equal to zero, due to numerical precision. Therefore we have selected only types *peak*, *pit*, *saddle valley* and *saddle ridge* for our analysis [15].

a) Amount of each Surface Type:
This measure indicates the relative frequency of each type of surface in the nodule, where APK (Amount of *peak* surface), API (Amount of *pit* surface), ASR (Amount of *saddle ridge* surface) and ASV (Amount of *saddle valley* surface).

b) Area Index for each Surface Type:
For each surface type, the area occupied in the nodule divided by the total nodule area is computed, where *AIPK* (Area Index for *peak* surface), *AIPI* (Area Index for *pit* surface), *AISR* (Area Index for *saddle ridge* surface) and *AISV* (Area Index for *saddle valley* surface).

c) Mean *Curvedness* for each Surface Type:
Curvedness is a positive number that measures the curvature amount or intensity on the surface [13]:

$$c = \sqrt{\frac{k_{\min}^2 + k_{\max}^2}{2}} \tag{6}$$

The measures are based on the *curvedness* and the surface types. For each surface type, the mean *curvedness* is determined using the *curvedness* of each surface type, divided by the *curvedness* number in each surface type. Where, *CPK* (mean *curvedness* for *peak*), *CPI* (mean *curvedness* for *pit*), *CSR* (mean *curvedness* for *saddle ridge*) and *CSV* (mean *curvedness* for *saddle valley*).

3 Classification Algorithm

The idea of classification is to encounter a path from the pattern presented to a known target, in the present case to a malignant or to a benign pattern. Furthermore the path found should be the shortest in some sense, in such way that the presented pattern seems to be nearer from a known target and therefore it can be considered of the type of the target. Considering the diverse techniques, the Reinforcement Learning (RL) was chosen to find this path, because it can learn without a mathematical model of a path and because it can learn a correct path only using a reward when the target is encountered [16]. The RL technique presents the following characteristics [17]: Intuitive data; Cumulative learning; and Direct knowledge acquisition.

The first characteristic says that the data manipulated should come from some physical measure or be easily understandable. The second one provides the knowledge to grow up while more data are processed. The last one permits an ease way to store the learning [17].

The RL technique works based on states and actions. The states are a set of variables, each one storing a value of a specific measure. The objective of the states is to configure some situation of an environment. For instance, a geometric figure can be characterized by the number of sides, the size of each side and the angle between each two sides, then for this case there are three different states.

Each set of states has a set of actions, whose objective is to provide a changing in the environment, in order to achieve the desired goal. For example, for a mobile robot in a room, the states can be the position and velocity of an obstacle in this room. The actions are: turn right and turn left. Hence, for a given position and velocity of an obstacle, the turn left action can be decided and for another set

of values from these states, to turn right is more adequate, all trying to achieve the goal, in this example to avoid the obstacle [18].

As explained, for each set of state values, there are some actions. Each action has a value, which is obtained during the training phase. This value is used to find the best action, normally the action with the greatest value. As a action can result in a bad or good experience, a (bad or good) reward is given to an action, when it is chosen. Then one can say that a good action taken produces good value for this action and a bad action, a bad value associated. So, a decision taken in the future is based on values, which are obtained in the past, this means that an action will be chosen based on past experiences, which are realized during the training phase. Therefore, in order to decide an action, the system identifies the actions corresponding to the present set of state values and chooses the action with the greatest value.

But how is obtained the values of each action? The values are obtained during the training. In this phase, many trials are executed to find a path from an initial point to the target. Each successful trial becomes a good reward. This reward is given only to the action chosen, but it can be spread out for the others action executed before. During the training, when an action is chosen, the value associated to this action - $Q(s_t, a_t)$ - is updated considering its present value, the reward obtained with this choice r - and the value of the best action, which will be chosen in the next step - $max_a(Q(s_{t+1}, a_{t+1}))$ -. So the action of the next step can make an influence in the present action, of course in the next trial. The following equation shows the Q-learning updating rule for an action [16].

$$Q(s_t, a_t) = Q(s_t, a_t) + \alpha(r + \gamma max_a(Q(s_{t+1}, a_{t+1})) - Q(s_t, a_t)) \quad (7)$$

The two parameters α and γ are, respectively, the learning rate and the discount rate. The last one is used to increase or not the influences of a previous action in the future actions, in such way that $\gamma = 0$ means one action decided now causes no influences in the next actions. Tha data structure Q is a matrix, where each cell correponds to a particular set of states and actions. For example, if the system has three states and two actions, then Q has five dimensions. To be used in a matrix, states and actions must be discretized using any method.

4 Tests and Results

This section shows the results obtained from the application of the RL to a set of lung nodules classification based on its 3D geometric characteristics, discriminanting them between malignant from benign.

The tests described in this paper were carried out using a sample of 36 nodules, 29 benign and 7 malignant. It is important to note that the nodules were diagnosed by physicians and had the diagnosis confirmed by means of surgery or based on their evolution. Such process takes about two years, which explains the reduced size of our sample. The sample included nodules with varied sizes and shapes, with homogeneous and heterogeneous characteristics, and in initial and advanced stages of development.

The stepwise analysis [19] selected 5 out of the 13 measures (states), described in Section 2.3, to be analyzed by the reinforcement learning classifier. The selected states were ICE, QPK, QSR, QSV e CPI. Each state was discretized in ten different values. Thus, an action increase, maintain or decrease the present value of the corresponding state, generating five different actions, one for each state. The discretization of each state is shown in Table 1.

State	ICE	QPK	QSR	QSV	CPI
1	45 - 492.61	9 - 145.88	5 - 167.55	23 - 369.83	0.24 - 0.27
2	492.61 - 1.39e+3	145.89 - 419.67	167.55 - 492.67	369.83 - 1.06e+3	0.27 - 0.32
3	1.39e+3 - 2.29e+3	419.67 - 693.44	492.67 - 817.78	1.06e+3 - 1.76e+3	0.32 - 0.37
4	2.28e+3 - 3.18e+3	693.44 - 967.22	817.77 - 1.14e+3	1.76e+3 - 2.45e+3	0.37 0.43
5	3.18e+3 - 4.07e+3	967.22 - 1,240	1.14e+3 - 1,467	2.45e+3 - 3.14e+3	0.43 - 0.48
6	4.07e+3 - 4.97e+3	1,241 - 1.51e+3	1,468 - 1.79e+3	3.14e+3 - 3.84e+3	0.48 - 0.53
7	4.97e+3 - 5.86e+3	1.51e+3 - 1.78e+3	1.79e+3 - 2.12e+3	3.84e+3 - 4.53e+3	0.53 0.58
8	5.86e+3 - 6.76e+3	1.79e+3 - 2.06e+3	2.12e+3 - 2.44e+3	4.53e+3 - 5.22e+3	0.58 0.64
9	6.76e+3 - 7.65e+3	2.06e+3 - 2.33e+3	2.44e+3 - 2.77e+3	5.22e+3 - 5.92e+3	0.64 - 0.69
10	7.65e+3 - 8,102	2.33e+3 - 2,473	2.77e+3 - 2,931	5.92e+3 - 6,266	0.69 - 0.719

Table 1. Discretization of each state.

With these states and actions, the matrix Q has the following size: 10^5x3^5, because each state has ten different values and each action three possibilities.

The training was made selecting nineteen images of benign nodules and four malignant, and we choose the more characteristic malignant and benign nodule as target. Each image was represented by the five states described above. During the training, each set of states of an image was used as start point of a trip to the target (malignant or benign). Each step of this trip consists of a set of actions, one for each state. One set of actions can be: increase the value of state 1, decrease the value of state 2, and so on. At the end of a trip, when the correct target is found (malignant or benign), the training system provided a reward of value one and zero for others points. After one trial, another trial was made using data of another image. A session training containing all images is an episode. In order to find out the best way, that means, the best action for each set of states, sometimes actions must be chosen randomly. So, in this research, initially the rate of random choice was 50%. The random choice of an action provides a test of another path to the target and posterior comparation with the previous paths.

After the training, the knowledge should have been acquired. This is verified with a test of classification with images not used during the training phase. For this purpose nine bening and two malignant images were selected.

Figure 3 shows the results obtained, where we used the remained nine benign and two malignant nodules. In this figure we represent in the x-axis the nodules case, being cases 1 to 9 benign and cases 10 and 11 malignant. On other hand, the y-axis represent the number of steps from they start point to the target, which means the number of actions taking to reach the case target. When a case take a positive number of steps to reach the target we have a successful

classification. Otherwise a negative number represents an incorrect classification and when the classification is not determined we set the number of steps as zero.

The obtained data was generated from four experiments, using 20000, 30000, 40000 and 50000 episodes in the training phase.

The number of right classification grows from 45% for 20000 episodes to 81% for 50000 episodes; as show in Table 2, which indicate a good improvement in the classification success as the number of episodes grows.

An interesting information observed in the results is for 40000 episodes, when the number of successful classification decreased, which should be derived from the random choices used in the training phase, that lead to a poor learning. But, as already proved in RL theorem [16], a very high number of episodes drives to a correct learning, generating a very high successful rate in the classification.

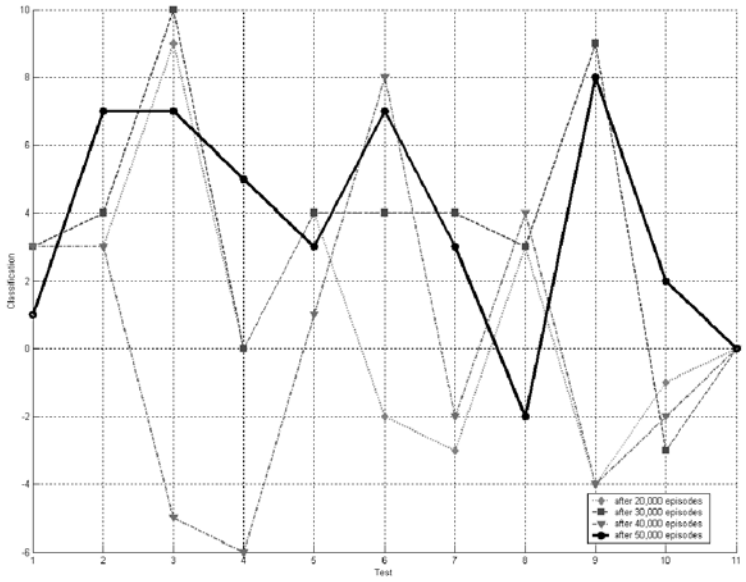

Fig. 3. Application of Reinforcement Learning technique.

Due to the relatively small size of the existing CT lung nodule databases and the various CT imaging acquisition protocols, it is difficult to compare the diagnosis performance between the developed algorithms and others proposed in the literature.

Success	Error	Non-Determined	Number of Episodes
45.45%	36.36%	18.18%	20,000
72.72%	9.09%	18.18%	30,000
45.45%	45.45%	9.09%	40,000
81.81%	9.09%	9.09%	50,000

Table 2. Application of Reinforcement Learning technique

5 Conclusion

This paper presented the use of reinforcement learning to solve the problem of lung nodules classification based on 3D geometrics characteristics.

The number of nodules studied in our dataset is too small and the disproportion in the samples does not allow us to make definitive conclusions, However, the results obtained with our sample are very encouraging, demonstrating that the reinforcement learning classifier using characteristics of the nodules' geometry can effectively classify benign from malignant lung nodules based on CT images. Nevertheless, there is the need to perform tests with a larger database and more complex cases in order to obtain a more precise behavior pattern.

Despite the good results obtained we should research to find out a way to shorter the training phase, while maintaining the learning quality. We also must improve our nodules database to generate more definitive results and to make possible the comparison with other classifiers.

Acknowledgments

We thank Dr. Rodolfo Nunes and his team for the clinical support, and Dr. Marcia Boechat with the staff of Instituto Fernandes Figueira, for the images.

References

1. Tarantino, A.B.: 38. In: Nódulo Solitário Do Pulmão. 4 edn. Guanabara Koogan, Rio de Janeiro (1997) 733–753
2. Henschke, C.I., et al: Early lung cancer action project: A summary of the findings on baseline screening. The Oncologist **6** (2001) 147–152
3. Reeves, A.P., Kostis, W.J.: Computer-aided diagnosis for lung cancer. Radiologic Clinics of North America **38** (2000) 497–509
4. Silva, A.C., Carvalho, P.C.P., Gattass, M.: Analysis of spatial variability using geostatistical functions for diagnosis of lung nodule in computerized tomography images. Pattern Analysis and Applications **7** (2005) 227–234
5. Silva, A.C., Carvalho, P.C.P., Gattass, M.: Diagnosis of solitary lung nodule using semivariogram and skeletonization in computerized tomography images. 21st Meeting of the Society for Computer Applications in Radiology (SCAR 2004) (2004)

6. Silva, A.C., Carvalho, P.C.P., Peixoto, A., Gattass, M.: Diagnosis of lung nodule using gini coefficient and skeletonization in computerized tomography images, NY, USA, ACM Press New York (2004) 243–248 19th ACM Symposium on Applied Computing (SAC 2004).
7. Clunie, D.A.: DICOM Structered Reporting. PixelMed Publishing, Pennsylvania (2000)
8. Nikolaidis, N., Pitas, I.: 3-D Image Processing Algorithms. John Wiley, New York (2001)
9. Lorensen, W.E., Cline, H.E.: Marching cubes: A high resolution 3D surface construction algorithm. Computer Graphics **21** (1987) 163–169
10. Ohtake, Y., Belyaev, A., Pasko, A.: Dynamic meshes for accurate polygonization of implicit surfaces with shape features. In Press, I.C.S., ed.: SMI 2001 International Conference on Shape Modeling and Applications. (2001) 74–81
11. Smith, A.C.: The Folding of the Human Brain, from Shape to Function. PhD thesis, University of London (1999) Available at http://carmen.umds.ac.uk/a.d.smith/phd.html.
12. Essen, D.C.V., Drury, H.A.: Structural and functional analyses of human cerebral cortex using a surface-based atlas. The Journal of Neuroscience **17** (1997) 7079–7102
13. Koenderink, J.J.: Solid Shape. MIT Press, Cambridge, MA, USA (1990)
14. Henderson, D.W.: Differental Geometry: A Geometric Introduction. Prentice-Hall, Upper Saddle River, New Jersey (1998)
15. Kawata, Y., Niki, N., , Ohmatsu, H., Kakinuma, R., Eguchi, K., Kaneko, M., Moriyama, N.: Classification of pulmonary nodules in thin-section CT images based on shape characterization. In: International Conference on Image Processing. Volume 3., IEEE Computer Society Press (1997) 528–530
16. Barto, A., Sutton, R., Anderson, C.: Neuronlike adaptive elements that can solve difficult learning control problems. IEEE Transactions on Systems, Man and Cybernetics **13** (1983) 834–846
17. Almeida, A., Heimann, B., Góes, L., Nascimento, C.: Obstacle avoidance in dynamic environment: A hierarchical solution. Volume 6., São Paulo, Congresso Brasileiro de Redes Neurais (2003) 289–294
18. Almeida, A., Heimann, B., Góes, L., Nascimento, C.: Avoidance of multiple dynamic obstacles. In: International Congress of Mechanical Engineering. Volume 17., São Paulo (2003)
19. Duda, R.O., Hart, P.E.: Pattern Classification and Scene Analysis. Wiley-Interscience Publication, New York (1973)